Bone 83 (2016) 210–219

Contents lists available at ScienceDirect

Bone

journal homepage: www.elsevier.com/locate/bone

Original Full Length Article

Factors secreted from dental pulp stem cells show multifaceted benefits for treating experimental rheumatoid arthritis

Jun Ishikawa [a], Nobunori Takahashi [b], Takuya Matsumoto [b], Yutaka Yoshioka [b], Noriyuki Yamamoto [a], Masaya Nishikawa [a], Hideharu Hibi [a], Naoki Ishigro [b], Minoru Ueda [a], Koichi Furukawa [c], Akihito Yamamoto [a,*]

[a] Department of Oral and Maxillofacial Surgery, 65 Tsurumai-cho, Showa-ku, Nagoya 466-8550, Japan
[b] Orthopedic Surgery and Rheumatology, 65 Tsurumai-cho, Showa-ku, Nagoya 466-8550, Japan
[c] Biochemistry II of Nagoya University Graduate School of Medicine, 65 Tsurumai-cho, Showa-ku, Nagoya 466-8550, Japan

ARTICLE INFO

Article history:
Received 3 July 2015
Revised 2 November 2015
Accepted 17 November 2015
Available online 19 November 2015

Keywords:
Dental pulp stem cells
Conditioned medium
Macrophages
Osteoclasts
Rheumatoid arthritis
Inflammation

ABSTRACT

Rheumatoid arthritis (RA) is an autoimmune disease characterized by synovial hyperplasia and chronic inflammation, which lead to the progressive destruction of cartilage and bone in the joints. Numerous studies have reported that administrations of various types of MSCs improve arthritis symptoms in animal models, by paracrine mechanisms. However, the therapeutic effects of the secreted factors alone, without the cell graft, have been uncertain. Here, we show that a single intravenous administration of serum-free conditioned medium (CM) from human deciduous dental pulp stem cells (SHED-CM) into anti-collagen type II antibody-induced arthritis (CAIA), a mouse model of rheumatoid arthritis (RA), markedly improved the arthritis symptoms and joint destruction. The therapeutic efficacy of SHED-CM was associated with an induction of anti-inflammatory M2 macrophages in the CAIA joints and the abrogation of RANKL expression. SHED-CM specifically depleted of an M2 macrophage inducer, the secreted ectodomain of sialic acid-binding Ig-like lectin-9 (ED-Siglec-9), exhibited a reduced ability to induce M2-related gene expression and attenuate CAIA. SHED-CM also inhibited the RANKL-induced osteoclastogenesis *in vitro*. Collectively, our findings suggest that SHED-CM provides multifaceted therapeutic effects for treating CAIA, including the ED-Siglec-9-dependent induction of M2 macrophage polarization and inhibition of osteoclastogenesis. Thus, SHED-CM may represent a novel anti-inflammatory and reparative therapy for RA.

1. Introduction

The precise etiology of rheumatoid arthritis (RA) remains unclear, however monocyte lineage cells, including macrophages and osteoclasts, respectively play central roles in the inflammation and bone resorption of RA [1,2]. Recent studies indicate that differentially activated macrophages are involved in the pathophysiology of various types of intractable diseases [3]. The pro-inflammatory M1 cells and anti-inflammatory M2 cells are thought to represent the extreme activation states on each end of a continuum [3–5]. Classically activated M1 cells initiate inflammation, promote osteoclast differentiation, and accelerate tissue damage by releasing high levels of pro-inflammatory cytokines, reactive oxygen species, and nitric oxide [6]. In contrast, M2 cells counteract pro-inflammatory M1 conditions by secreting anti-inflammatory cytokines and scavenging cellular debris. In general wound repair, M1- and M2-like cells are involved in initiating and resolving inflammation, respectively [7]. Thus, strategies designed to modulate macrophage polarity may provide significant therapeutic benefits for RA.

Stem-cell transplantation represents a new therapeutic strategy for treating RA [8,9]. The transplantation of mesenchymal stem cells (MSCs) derived from bone marrow [10], adipose tissue [11], umbilical cord [12], or gingival tissue [13] improves arthritis symptoms in mouse models of RA *via* paracrine, trophic, and/or immunomodulatory mechanisms. However, the therapeutic effects of soluble factors secreted from various types of MSCs have not been reported.

Human adult dental pulp stem cells (DPSCs) and stem cells from human exfoliated deciduous teeth (SHEDs) are self-renewing MSCs residing within the perivascular niche of the dental pulp [14–16]. These cells are thought to originate from the cranial neural crest, and express both MSC and neural stem cell markers [17]. Studies of engrafted SHEDs and DPSCs in various animal disease models, including myocardial infarction [18], systemic lupus erythematosus [19], ischemic brain injury [20,21], and spinal cord injury [17–22,23], demonstrated that these cells can promote significant recovery through paracrine mechanisms, which enhance endogenous tissue-repairing activities [24]. We recently reported the therapeutic effects of intrathecally administered serum-free conditioned medium derived from SHED (SHED-CM) for severe spinal cord injury in rat. The efficacy of SHED-CM was associated with an immunoregulatory activity that induced anti-inflammatory M2-like macrophages through the synergistic action of monocyte chemoattractant

* Corresponding author at: 65 Tsurumai-cho, Showa-ku, Nagoya 466-8550, Japan.
E-mail address: akihito@med.nagoya-u.ac.jp (A. Yamamoto).

http://dx.doi.org/10.1016/j.bone.2015.11.012
8756-3282/

Table 1
Mouse primers for real time q-PCR.

Primer	Sequence (forward 5′–3′)	Sequence (reverse 5′–3′)
GAPDH	AACTTTGGCATTGTGGAAGG	GGATGCAGGGATGATGTTCT
TRAP	TCCTGGCTCAAAAAGCAGT	ACATAGCCCACACCGTTCTC
Cathepsin K	CAGCAGAGGTGTGTACTATG	GCGTTGTTCTTATTCCGAGC
NFATc1	CGGGAAGAAGATGGTGCTGT	TTGGACGGGGCTGGTTAT
RANK	CGAGGAAGATTCCCACAGAG	CAGTGAAGTCACAGCCCTCA
RANKL	ATGAAAGGAGGGAGCACGAA	GGAAGGGTTGGACACCTGAA
TNF-α	CCCTTTACTCTGACCCCTTTATTGT	TGTCCCAGCATCTTGTGTTTCT
IL-1β	AGTTGACGGACCCCAAAAGA	ACAGCTTCTCCACAGCCACA
IL-6	CCAAGAACGATAGTCAATTCCAGA	CATCAGTCCCAAGAAGGCAAC
iNOS	AGCCAAGCCCTCACCTACTTC	GCCTCCAATCTCTGCCTATCC
MMP3	GGCCTGGAACAGTCTTGGC	TGTCCATCGTTCATCATCGTCA
MMP9	GGACCCGAAGCGGACATTG	CGTCGTCGAAATGGGCATCT
F4/80	CCAGAAGGCTCCCAAGGAT	TCTGCTCACTTTGGAGTATCAAGTC
CD206	TCTCCCGGAACCGACTCTTC	AACTGGTCCCCTAGTGTACGA
Arginase1	CTCCAAGCCAAAGTCCTTAGAG	AGGAGCTGTCATTAGGGACATC
Fizz1	CCAATCCAGCTAACTATCCCTCC	CCAGTCAACGAGTAAGCACAG

protein-1 (MCP-1) and the secreted ectodomain of sialic acid-binding Ig-like lectin-9 (ED-Siglec-9) in SHED-CM [25]. However, the therapeutic potential of SHED-CM for RA has not been examined.

Here, we examined the therapeutic benefits of SHED-CM for arthritis induced by an anti-collagen type II antibody (CAIA). CAIA is a rapid arthritis model, which represents the effector phase of arthritis. Our data showed that SHED-CM improved arthritis symptoms and inhibited tissue damage by inducing M2 macrophage polarization in CAIA mice. Our findings suggested that SHED-CM has multiple therapeutic anti-inflammatory effects and inhibits osteoclastogenesis in mice. Thus, SHED-CM may represent a novel and powerful approach for treating RA and other inflammatory and autoimmune diseases.

2. Materials and methods

2.1. Cells

Human SHEDs were isolated as described previously [16,17]. Briefly, exfoliated deciduous teeth (from 6- to 12-year-old individuals) were collected at Nagoya University Hospital, under approved guidelines set by Nagoya University (H-73, 2003). Ethical approval was obtained from the Ethics Committee of Nagoya University (permission number 8-2). All study participants provided written informed consent. After separating the crown and root, the dental pulp was isolated and then digested in a solution containing 3 mg/ml collagenase type I and 4 mg/ml dispase for 1 h at 37 °C. Single-cell suspensions ($1–2 \times 10^4$ cells/ml) were plated on culture dishes in DMEM supplemented with 10% fetal bovine serum, then incubated at 37 °C in a humidified atmosphere of 5% CO_2.

BMSCs (from 20- to 22-year-old individuals) at passage 5 were obtained from Lonza.

Table 2
Therapeutic factors in SHED-CM for RA.

	Ratio (vs DMEM)	Ratio (vs BMSC-CM)	References
Immunosuppression			
HGF	23.28	3.21	29
IL-22	10.20	3.31	30
Furin	3.88	3.18	33
Anti-inflammation			
IL-1Ra	0.93	0.94	31
RAGE	1.67	1.96	32
Anti-osteoclastogenesis			
OPG	412.05	3.70	28
Macrophage differentiation			
MCP-1	120.25	1.54	25
ED-siglec-9	2.08	1.79	25

2.2. Preparation of conditioned medium (CM)

At passage 5–9, SHEDs or BMSCs at 70–80% confluence were washed with PBS and serum-free DMEM for two times, then the culture medium was replaced with DMEM. After 48 h incubation at 37 °C in a humidified atmosphere of 5% CO_2, the medium was collected and centrifuged for 3 min at 440 *g* at 4 °C. The supernatants were collected and centrifuged for 3 min at 1750 *g* at 4 °C. The supernatants were used as CM for CAIA treatment or assays.

2.3. Animals

Male 8-week-old DBA/1 J mice were obtained from Japan SLC. The animals were housed in plastic cages (4 mice per cage), with wood tip bedding, and maintained under specific pathogen-free conditions in a temperature- and humidity-controlled room (23 ± 2 °C and 55 ± 10%, respectively) under a fixed 12 h light/dark cycle (9:00 a.m. to 9:00 p.m.). The animals were given free access to standard laboratory food and water. The animal experiments were performed in accordance with the Guidelines for Animal Experimentation of Nagoya University School of Medicine.

2.4. Induction of arthritis and experimental design

The arthritogenic mouse anti-collagen type II monoclonal antibody (mAb) cocktail (Chondrex), contains equal amounts of 5 mAbs (A2-10, F10-21, D8-6, D1-2G, and D2-112). On day 0, the mice were intraperitoneally injected with 1.5 mg of the cocktail. On day 3, the mice were intraperitoneally injected with 50 μg of lipopolysaccharide (LPS). On day 5, 500 μl of SHED-CM, BMSC-CM, or serum-free DMEM was injected into the tail vein of CAIA mice. On day 7 or 14, at least five mice per treatment group were sacrificed under deep anesthesia. From days 0 to 14, the mice were blindly inspected for disease progression (Fig. 1A).

2.5. Arthritis evaluation

From days 0 to 14, the mice were blindly inspected for disease progression. The severity of arthritis in each paw was graded on a scale of 0–4, as follows: 0, normal; 1, mild swelling; 2, moderate swelling; 3, severe swelling; 4, pronounced edema of the entire paw. The cumulative score from 4 paws (maximum score of 16 per mouse) was used as the overall disease score.

2.6. Histology

On day 14, the mice were sacrificed and the hind paws were fixed in 4% paraformaldehyde, decalcified in 10% EDTA for 3 weeks, and embedded in paraffin. Serial 5-μm sections were stained with hematoxylin and eosin (H–E) and toluidine blue, and stained for tartrate-resistant acid phosphatase (TRAP) using a leukocyte acid phosphatase kit according to the manufacturer's instructions (Sigma-Aldrich).

2.7. Histological scoring

The samples were evaluated for synovial inflammation, bone erosion, and cartilage damage in a blinded manner, as described previously, with minor modifications [26].

Synovial inflammation was scored as follows: 0, no inflammation; 1, slight thickening of the lining layer with some infiltrating cells in the sublining layer; 2, moderate thickening of the lining layer with a moderate number of infiltrating cells in the sublining layer; 3, extensive thickening of the lining layer with a moderate number of infiltrating cells in the sublining layer and the presence of inflammatory cells in the synovial space; 4, substantial influx of inflammatory cells into the synovium.

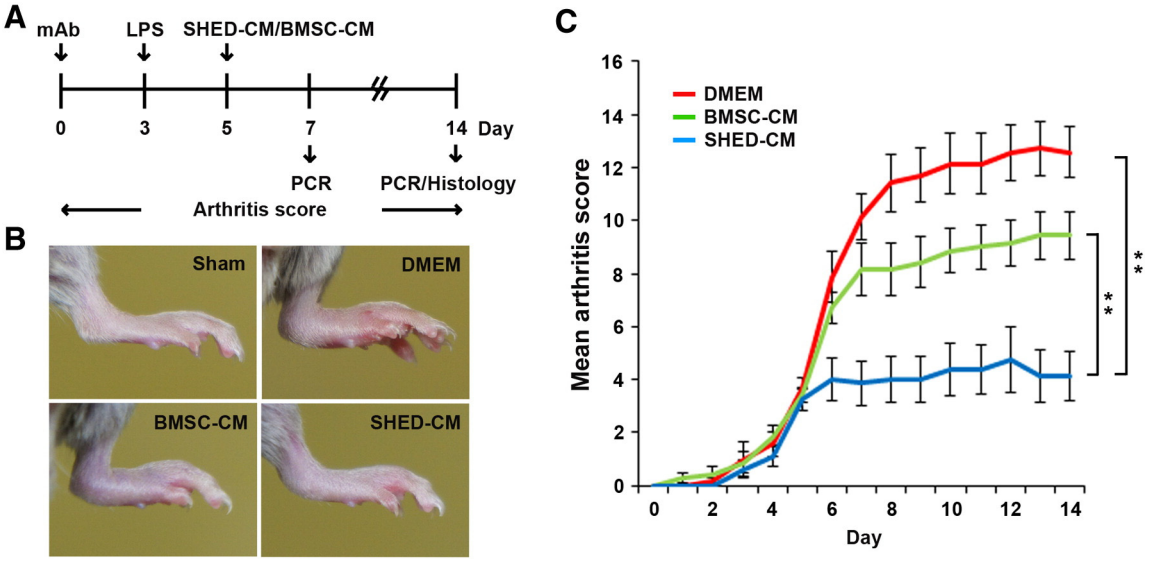

Fig. 1. SHED-CM treatment improves disease severity in CAIA mice. (A) Experimental design. mAb: anti-collagen type II monoclonal antibody, LPS: lipopolysaccharide. (B) Representative images of a hind paw on day 14. (C) Disease scores of CAIA mice treated with DMEM, BMSC-CM, or SHED-CM ($n = 8$ per group). Arthritis symptoms were evaluated by a blinded independent observer for up to 14 days following mAb injection. Data represent the mean ± SEM; $^{**}p < 0.01$.

Bone erosion was scored as follows: 0, no erosion; 1, small areas of resorption not readily apparent in the trabecular or cortical bone; 2, numerous areas of resorption, readily apparent in the trabecular or cortical bone at low magnification; 3, obvious resorption of the trabecular and cortical bone without full-thickness defects in the cortex, but with the loss of some trabecular bone; 4, full-thickness defects in the cortical bone and marked loss of trabecular bone with no distortion of the remaining cortical surface; and 5, full-thickness defects in the cortical and trabecular bone with distortion of the remaining cortical surface.

Cartilage damage was scored as follows: 0, no destruction; 1, minimal erosion; 2, slight to moderate erosion in a limited area; 3, extensive erosion; and 4, general destruction.

The cumulative score for the 2 hind paws was used as the histological arthritis score, resulting in maximum scores of 8, 10, and 8 respectively for synovial inflammation, bone erosion, and cartilage damage.

2.8. Immunohistochemistry

On day 7, the hind paws were harvested, embedded in SCEM gel (8091140; Leica), and frozen in cooled isopentane. Non-decalcified hind paw sections were generated using Kawamoto's film method (8091098; Leica) [27]. The sections were fixed in 99.5% ethanol for 10 min at room temperature, washed, permeabilized with 0.1% (*v*/*v*) Triton X-100 in PBS for 20 min, blocked with 5% bovine serum albumin/PBS for 30 min, and stained with primary antibodies in blocking buffer for overnight at 4 °C. The sections were then stained with secondary antibodies for 30 min, mounted with an SCMM R3 (Leica), and examined with a fluorescence microscope (BZ9000; Keyence). The following antibodies were used for immunostaining: rat monoclonal antibody against F4/80 (ab6640; Abcam), rabbit polyclonal antibody against iNOS (ab3523; Abcam), rabbit polyclonal antibody against CD206 (ab64693; Abcam). Secondary antibodies were conjugated with Alexa Fluor 546 or 647 (Invitrogen). Cell nuclei were labeled with 4′, 6-diamidino-2-phenylindole (DAPI) (Invitrogen).

2.9. RNA preparation and real-time q-PCR analysis

Total RNA from paws on day 7 or 14 was quantified by a spectrophotometer, and RNA integrity was checked on 1% agarose gels. Reverse transcription reaction was carried out with Superscript III reverse transcriptase (Invitrogen) using 0.5 μg of total RNA in a 25-μl total reaction volume. Real-time q-PCR was performed using the THUNDERBIRD SYBR qPCR Mix (Toyobo) and the StepOnePlus Real-Time PCR System (Applied Biosystems). Primers were designed using DNA Dynamo (Blue Tractor Software Ltd) and primer 3 (Table 1).

2.10. Osteoclast differentiation assay

Bone marrow cells were isolated from the femurs of 8-week-old male DBA/1 J mice using an established protocol [28]. They were seeded into 48-well plates at 1.5×10^5 cells/well in αMEM supplemented with 50 ng/ml M-CSF (R&D Systems) at 37 °C in a humidified atmosphere with 5% CO_2. After 3 days of incubation, the medium was replaced with serum-free DMEM, SHED-CM or BMSC-CM, which were supplemented with 50 ng/ml M-CSF and 100 ng/ml soluble RANKL (PeproTech). After 3 days of incubation, the cells were stained using a TRAP/ALP Stain Kit (Wako). TRAP-positive and multinuclear cells were counted under brightfield microscopy. TRAP-positive cells with ≥3 nuclei were defined as osteoclast-like cells. To evaluate bone-resorbing activity in osteoclast-like cells, pit formation assay was performed. Bone marrow cells were seeded into Osteo Assay 96-well Plate (CORNING) at 6×10^4 cells/well in αMEM supplemented with 50 ng/ml M-CSF at 37 °C in a humidified atmosphere with 5% CO_2. After 3 days of incubation, the medium was replaced with serum-free DMEM, SHED-CM or BMSC-CM, which were supplemented with 50 ng/ml M-CSF and 100 ng/ml soluble RANKL. After 7 days of incubation, von Kossa stain was performed and analyzed under bright-field microscopy.

2.11. CM cytokine measurements and protein depletion assay

The levels of osteoprotegerin (OPG) and Siglec-9 in CMs were determined by ELISA (Human OPG DuoSet ELISA Development System [R&D Systems]; RayBio Human Siglec-9 ELISA Kit [Raybiotech]). To deplete the Siglec-9 from SHED-CM, anti-Siglec-9 antibody (Abcam) prebound to Protein G Sepharose (GE Healthcare) was incubated with SHED-CM overnight at 4 °C, and then the antibody beads were removed by centrifugation. The loss of Siglec-9 from the SHED-CM was confirmed by ELISA.

2.12. M2 macrophage induction assay

Bone marrow cells were isolated from the femurs of 8-week-old male DBA/1 J mice. They were seeded into 24 well-plate at 3×10^5 cells/well and differentiated into macrophages in DMEM supplemented with 20 ng/ml M-CSF at 37 °C in 5% CO2 for 7 days. Then, the macrophages were incubated with serum-free DMEM, BMSC-CM, SHED-CM, or d-SHED-CM. After 24 h incubation, immunohistochemical analysis was carried out and the RNA extraction was performed using RNeasy micro kit (Qiagen).

2.13. Statistics

An unpaired 2-tailed Student's t-test was used for single comparisons. To analyze more than three independent groups, repeated-measures ANOVA with Tukey's post hoc test was used (SPSS 22.0). *P*-values less than 0.05 were considered statistically significant.

3. Results

3.1. A single intravenous injection of SHED-CM ameliorates the clinical symptoms of CAIA

To examine the therapeutic effects of SHED-CM for arthritis, we used the anti-CII mAb-induced arthritis (CAIA) mouse model (Fig. 1A). SHED- and BMSC- CMs were collected 48 h after culture in DMEM. The characteristics of the SHEDs and BMSCs were described previously [17] and see Methods. There were no significant differences between the SHEDs and BMSCs survival after incubation in serum-free DMEM *versus* that in serum-containing DMEM (data not shown). CAIA mice typically develop paw swelling around day 4 after the intraperitoneal injection of anti-CII mAb, followed by further exacerbation thereafter. After confirming early arthritis symptoms on day 5, the CAIA mice were treated with a single intravenous injection of SHED-CM, BMSC-CM, or DMEM. By day 8, DMEM- and BMSC-CM-treated mice respectively displayed severe and moderate swelling encompassing the ankle, foot, and digits. Notably, the SHED-CM-treated mice exhibited minimal paw swelling (Figs. 1B and C. Arthritis scores on day 8: DMEM, 11.43 ± 1.09; BMSC-CM, 8.14 ± 0.99; SHED-CM, 4.00 ± 0.87; $P < 0.01$ SHED-CM *versus* DMEM or BMSC-CM). No adverse effects were observed during the experimental period.

3.2. SHED-CM prevents tissue destruction in CAIA mice

Histological analysis (performed on day 14) of the ankle joints of DMEM-treated mice showed profound tissue damage, including synovial hyperplasia, inflammatory cell infiltration, pannus formation, and intense bone and cartilage destruction. Milder tissue destruction was observed in the BMSC-CM-treated mice. In contrast, SHED-CM-treated mice exhibited markedly reduced synovial inflammation and bone and cartilage destruction (Fig. 2A). The quantitative histological scores of synovial inflammation, bone erosion, and cartilage damage [26] were all significantly lower in SHED-CM-treated mice than in the BMSC-CM- or DMEM-treated mice (Fig. 2B).

3.3. SHED-CM inhibits osteoclastogenesis

The accumulation of large numbers of TRAP-positive osteoclasts was evident in the joints of the DMEM treatment groups on day 14, but was significantly suppressed in the SHED-CM group (Fig. 3A,B). In addition,

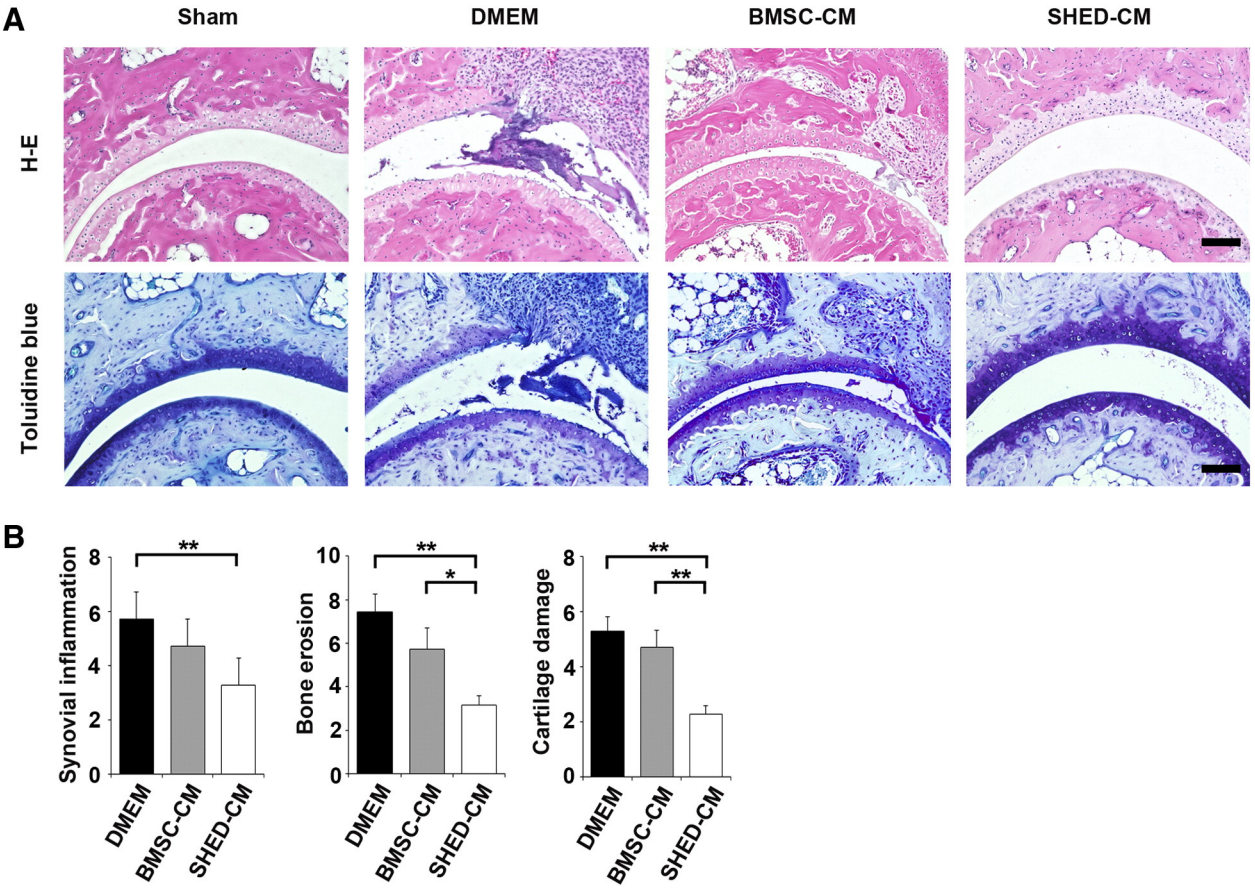

Fig. 2. SHED-CM attenuates tissue destruction in CAIA mice. (A) Representative microscopic images of the ankle joints obtained from sham, DMEM-, BMSC-CM-, and SHED-CM-treated mice on day 14 ($n = 8$ per group). Serial sections were stained with H-E and toluidine blue. Bar = 100 μm. (B) The histological scores for synovial inflammation, bone erosion, and cartilage damage were evaluated by a blinded independent observer. Data represent the mean ± SEM; $^*p < 0.05$, $^{**}p < 0.01$.

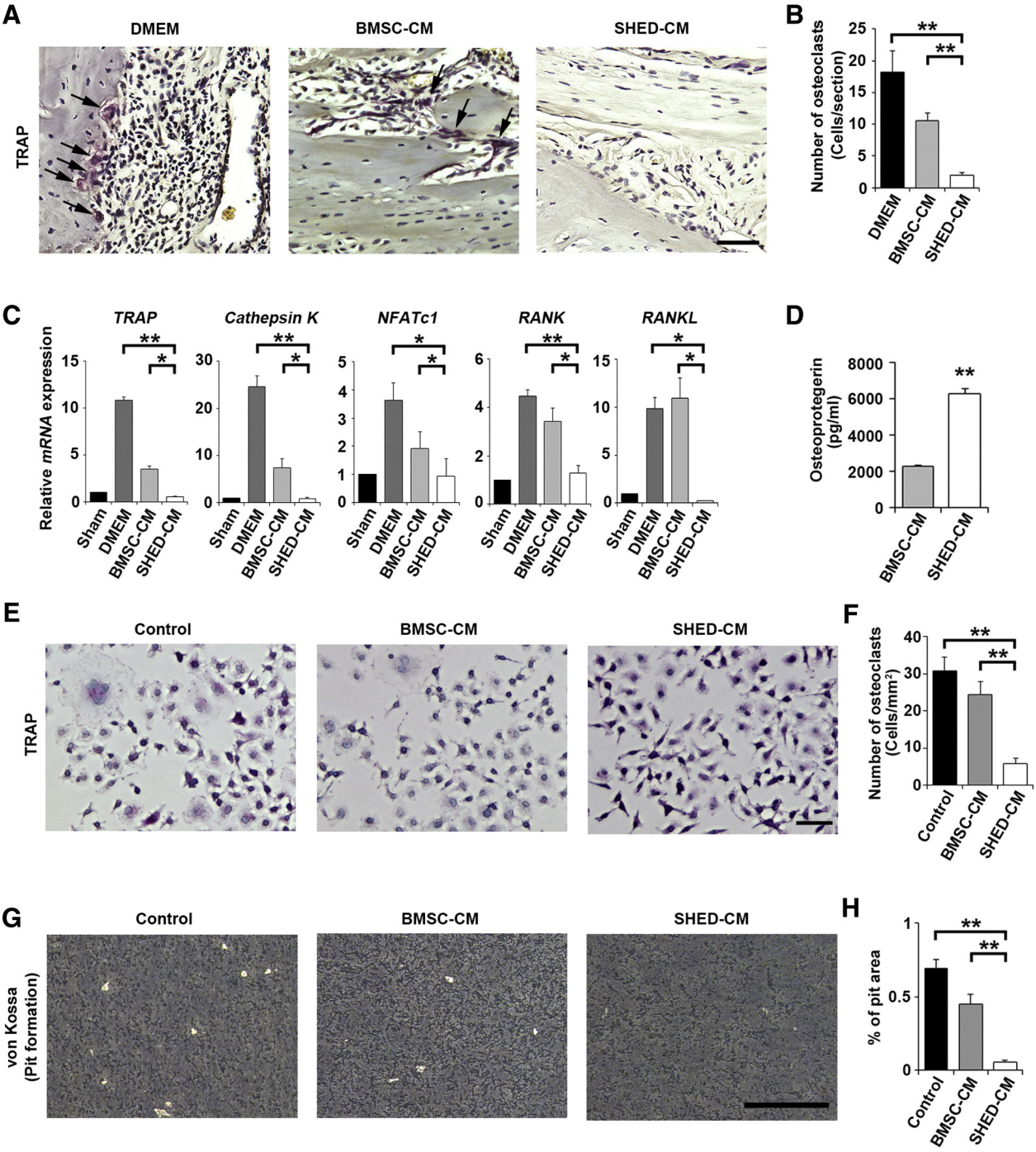

Fig. 3. SHED-CM inhibits *in vivo* and *in vitro* osteoclastogenesis. (A) Representative microscopic images of the ankle joints from DMEM-, BMSC- and SHED-CM-treated mice on day 14. Serial sections were stained for TRAP. Bar = 50 μm. (B) Quantification of the TRAP-positive cells in the ankle joints ($n = 5$ per group). Data represent the mean ± SEM; $^{**}p < 0.01$. (C) Expression of osteoclast-related genes (*TRAP*, *Cathepsin K*, *NFATc1*, *RANK*, and *RANKL*) in paws obtained from DMEM-, BMSC-CM-, and SHED-CM-treated mice on day 14 ($n = 5$ per group). Data represent the mean ± SEM; $^{*}p < 0.05$, $^{**}p < 0.01$. (D) Osteoprotegerin levels in the BMSC-CM or SHED-CM measured by ELISA. Data represent the mean ± SEM; $^{**}p < 0.01$. (E–F) Effect of BMSC-CM, and SHED-CM on osteoclastogenesis *in vitro* ($n = 5$ per group). (E) Representative microscopic images and (F) quantification of the TRAP-positive cells. Data represent the mean ± SEM; $^{**}p < 0.01$. Bar = 100 μm. (G-H) Evaluation of bone-resorbing activity of osteoclasts affected by DMEM, BMSC-CM, and SHED-CM *in vitro* ($n = 5$ per group). (G) Representative microscopic pit formation images. Pits were emphasized with von Kossa staining and (H) the percentage of pit area in relation to the total surface area was calculated. Data represent the mean ± SEM; $^{**}p < 0.01$. Bar = 100 μm.

SHED-CM abolished the expression of both osteoclast-inducing genes (*RANKL*) and osteoclast-specific genes (*TRAP*, *Cathepsin K*, *RANK*, *NFATc1*) in the joints. The BMSC-CM-mediated suppression was considerably weaker than that of SHED-CM (Fig. 3C).

Next, we examined the concentration of osteoprotegerin (OPG), a RANKL decoy receptor, in the SHED-CM. Human BMSCs constitutively produce OPG, resulting in the inhibition of osteoclastogenesis and of *NFATc1* and *Cathepsin K* expression in the absence of cell–cell contact [29]. ELISAs revealed that the OPG level in the SHED-CM was 2.8 times that in the BMSC-CM (Fig. 3D). Next, to investigate the direct effect of the CMs on osteoclastogenesis *in vitro*, bone marrow cells (BMCs) were cultured in the presence of SHED-CM, BMSC-CM, or serum-free DMEM (Control) under osteoclast differentiation conditions (in the presence of RANKL and M-CSF). BMCs cultured in BMSC-CM or DMEM

differentiated into multinucleated giant osteoclasts, whereas SHED-CM-treated cells underwent reduced osteoclast differentiation and exhibited a uniquely elongated morphology (Fig. 3E). The number of TRAP-positive osteoclasts was also significantly reduced in the SHED-CM group (Fig. 3F). To evaluate the bone-resorbing activity of osteoclasts, we performed the pit formation assay with von Kossa staining. The area and number of pit in SHED-CM were smaller significantly, compared to DMEM and BMSC-CM (Fig. 3G, H).

3.4. SHED-CM induces anti-inflammatory M2-type circumstances in the joints of CAIA

Two days after CM injection, we evaluated the levels of mRNAs encoding M1-related mediators, including pro-inflammatory cytokines (*TNF-α*, *IL-1β*, *IL-6*), inducible nitric oxide synthases (*iNOS*), and synovial fibroblasts (SFs)-related matrix metalloproteinases (*MMP3 and MMP9*) in the paws. Both the SHED-CM and BMSC-CM treatment groups showed significantly suppressed levels of the M1-related gene expression, compared to the DMEM group (Fig. 4A). The pan macrophage marker, *F4/80*, was also significantly reduced in the SHED-CM group (Fig. 4B). To evaluate M2 marker expression, each marker's level was normalized to that of *F4/80*. Notably, M2-related genes (*CD206*, *Arginase1*, and *Fizz1*) were up-regulated significantly in the SHED-CM group (Fig. 4B).

3.5. ED-Siglec-9-depleted SHED-CM fails to suppress CAIA

We recently showed that SHED-CM contains the M2-inducing factors MCP-1 and ED-Siglec-9, and that the depletion of either of these molecules abrogates the SHED-CM's ability to induce M2-like macrophages *in vivo* [25]. To determine the role of ED-Siglec-9 in SHED-CM-mediated improvement in the CAIA model, we prepared d-SHED-CM by immuno-depleting ED-Siglec-9 from SHED-CM (Fig. 5A). d-SHED-CM-treated mice exhibited increased CAIA severity compared to SHED-CM-treated mice (CAIA scores on day 8: DMEM, 11.67 ± 0.56; d-SHED-CM, 8.71 ± 1.02; SHED-CM, 4.13 ± 0.69; $P < 0.01$ SHED-CM *versus* DMEM or d-SHED-CM; Fig. 5B). The histological scores were significantly higher in the d-SHED-CM treatment group than in the SHED-CM group (Figs. 5C and D). In addition, mRNA analysis of the joints revealed that d-SHED-CM failed to induce M2 marker expression, (Figs. 6A and B). These results suggest that ED-Siglec-9 induced the expression of M2-related mediators and played an essential role in the SHED-CM-mediated abrogation of CAIA.

3.6. SHED-CM induces the M2 macrophages in vivo and in vitro

We immunohistologically examined the SHED-CM-mediated M2 macrophage induction. Both SHED-CM and BMSC-CM group reduced the proportion of $iNOS^+F4/80^+$ M1 cells, compared to the DMEM or d-SHED-CM groups (Fig. 7A). Notably, the proportion of $CD206^+F4/80^+$ M2 cells was increased in the SHED-CM group, but not BMSC-CM one (Fig. 7B).

We next examined whether SHED-CM was sufficient to induce the M2 differentiation of BMCs *in vitro*. It has been reported that the M2 macrophages derived from BMCs display elongated shapes compared to M1 macrophages [30]. We found that BMCs maintained spherical cell shapes in DMEM or d-SHED-CM, while BMCs in SHED-CM were elongated cell shapes (Fig. 8A). Immunohistochemical analysis revealed that the number of $CD206^+$ macrophages was increased significantly in SHED-CM, compared to DMEM, BMSC-CM, or d-SHED-CM (Fig. 8A). In addition, mRNA analysis displayed that the M2-related genes, *CD206*, *Arginase1*, were up-regulated significantly in SHED-CM (Fig. 8B).

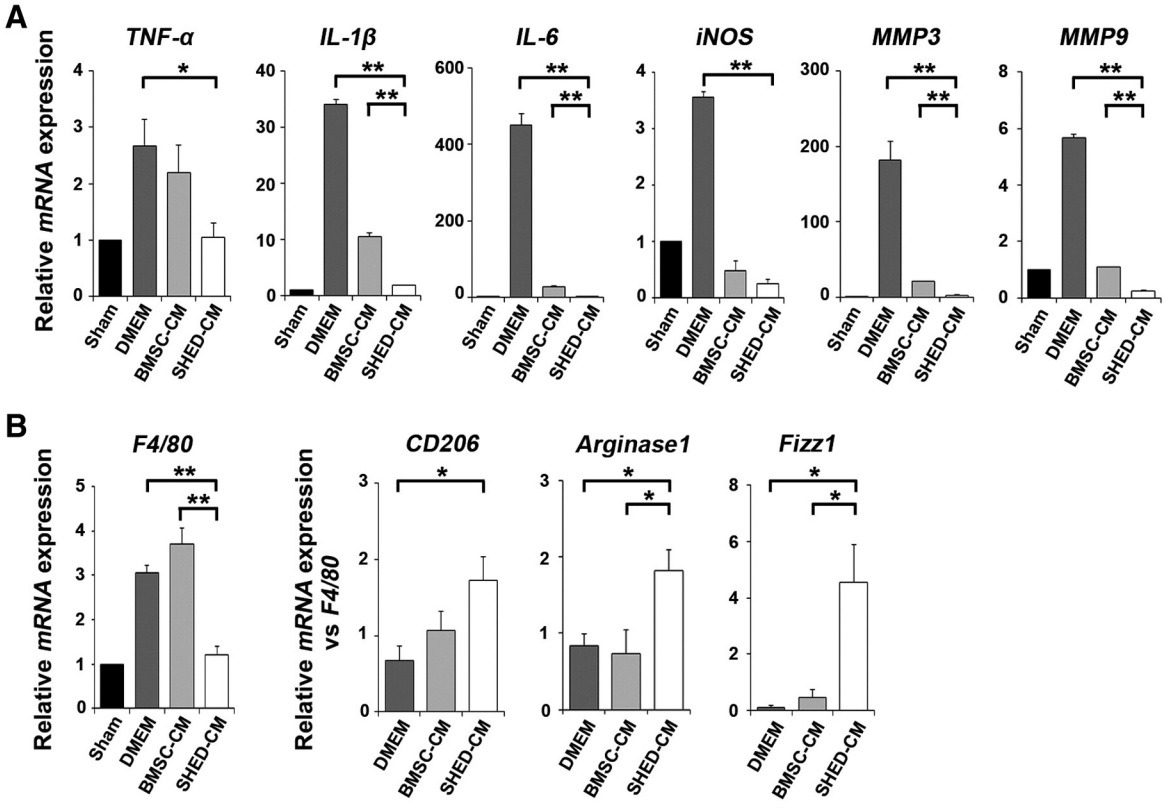

Fig. 4. SHED-CM suppresses inflammation and induces anti-inflammatory M2-related gene expressions. Gene expressions in paws obtained from DMEM-, BMSC-CM-, and SHED-CM-treated mice on day 7 ($n = 5$ per group). Data represent the mean ± SEM; $^*p < 0.05$, $^{**}p < 0.01$. (A) Pro-inflammatory cytokine (*TNF-α*, *IL-1β*, *IL-6*), *iNOS*, and *MMP* expressions. The results were normalized to that of the sham group. (B) Expression of *F4/80*, a pan macrophage marker and M2-related markers (*CD206*, *Arginase1*, and *Fizz1*). *F4/80* expression was normalized to that of the sham group, and M2-related markers were normalized to the *F4/80* expression in each sample.

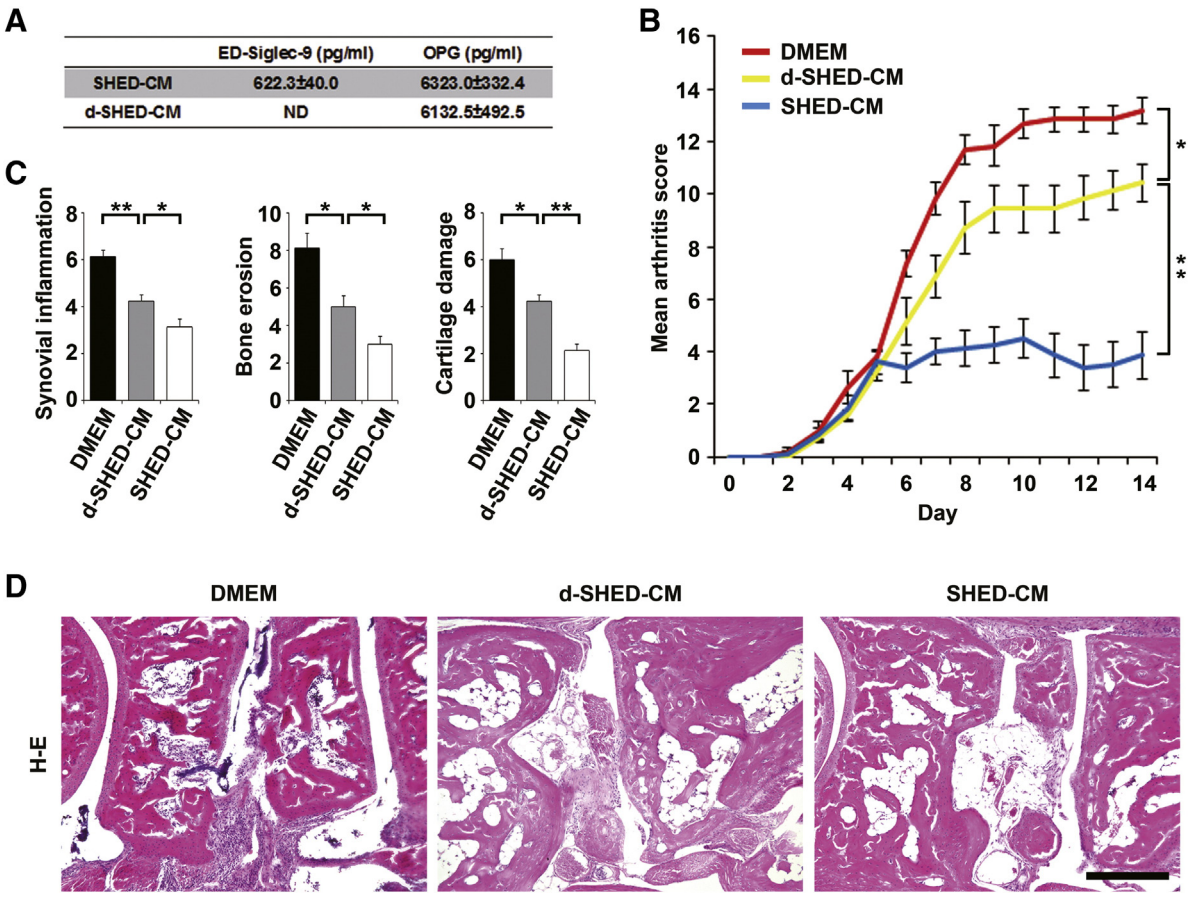

Fig. 5. d-SHED-CM fails to ameliorate arthritis symptoms and tissue destruction in CAIA (A) ED-Siglec-9 and OPG levels in SHED-CM and d-SHED-CM were measured by ELISA ($n = 5$ per group). Data represent the mean ± SEM. (B) Disease scores of CAIA mice treated with DMEM, d-SHED-CM, or SHED-CM ($n = 8$ per group). Arthritis symptoms were evaluated by a blinded independent observer for up to 14 days after mAb injection. Data represent the mean ± SEM; $^{*}p < 0.05$, $^{**}p < 0.01$. (C) Histological scores for synovial inflammation, bone erosion, and cartilage damage as evaluated by a blinded independent observer. Data represent the mean ± SEM; $^{*}p < 0.05$, $^{**}p < 0.01$. (D) Representative microscopic images of ankle joints obtained from DMEM-, d-SHED-CM-, or SHED-CM-treated mice on day 14 ($n = 8$ per group). Serial sections were stained with H-E. Bar = 300 μm.

4. Discussion

Numerous studies have reported that the intravenous infusion or intraarticular transplantation of various types of MSCs improves arthritis symptoms in animal models, by paracrine mechanisms. However, the therapeutic effects of the secreted factors alone, without the cell graft, have been uncertain. Here, we report for the first time, to our knowledge, the therapeutic potential of stem cell-derived CM for treating RA. A single intravenous administration of SHED-CM after CAIA onset prevented the exacerbation of arthritis symptoms. SHED-CM shifted the pro-inflammatory synovial environment toward an anti-inflammatory one by reducing the expression of mRNAs encoding M1-related cytokines, iNOS, and tissue-damaging proteases, and increasing the expression of anti-inflammatory M2-related genes. The resulting synovial environment suppressed osteoclastogenesis and the subsequent joint destruction of CAIA. Furthermore, SHED-CM directly inhibited the RANKL-mediated osteoclast development of bone marrow cells. Taken together, our findings suggest that SHED-CM may provide therapeutic benefits for RA.

We recently characterized the soluble factors in SHED-CM by cytokine antibody array analysis and found that SHED-CM contained 79 of the array proteins at more than 1.5 times the level in control DMEM [25]. Here, we performed a cluster analysis of these proteins, and identified 6 with known functional properties that may be beneficial in treating RA (Table 2). Hepatocyte growth factor (HGF) potently inhibits collagen-induced arthritis (CIA) development by augmenting the Th2-type response, which up-regulates IL-10 but down-regulates IL-17 production from Th17 cells [31]. Similarly, IL-22 reduces the severity of experimental arthritis by increasing IL-10 expression [32]. The IL-1 receptor antagonist (IL-1Ra) suppresses IL-1 signaling, which plays a critical role in joint inflammation and bone destruction [33]. Receptor for advanced glycation end products (RAGE) reduces pro-inflammatory cytokine expression in CIA joints [34], and Furin prevents arthritis by restoring the Th1/Th2 balance in the joint [35]. OPG, a decoy receptor for RANKL, inhibits osteoclastogenesis [29]. The combination of MCP-1 and ED-Siglec-9 synergistically promotes M2-like cell differentiation through the MCP-1 receptor, CCR2 [25]. Although the concentrations of these factors in SHED-CM were low (data not shown), we believe that their combinatorial effects could provide therapeutic benefits for RA. In addition, the deposition of hyaluronan in hyperplastic extracellular matrix is a peculiar characteristic of RA [36]. It has been shown that ED-Siglec-9 bind to the deposited hyaluronan [37]. We speculate that ED-Siglec-9 in SHED-CM also may bind to the joint hyaluronan. This would increase the local concentration of ED-Siglec-9, which accelerates M2 differentiation of synovial macrophages.

Our data showed that the SHED-CM-mediated improvement in arthritis was associated with the induction of M2 anti-inflammatory conditions in CAIA joints. Notably, d-SHED-CM or BMSC-CM (which lacks M2-inducing activity [25]), exhibited reduced therapeutic efficacy. These results are consistent with previous findings showing a central role for M2 cell induction in SHED-CM-mediated improvement in several animal models, including acute rat spinal cord injury [25], bleomycin-induced lung fibrosis [38], and fulminant hepatic failure (Matsushita, Y. *et al.*, unpublished observation). M2 macrophages counteract pro-inflammatory M1 conditions by secreting factors that promote cell survival, axonal regeneration, and neovascularization, and inhibit fibrosis. Collectively,

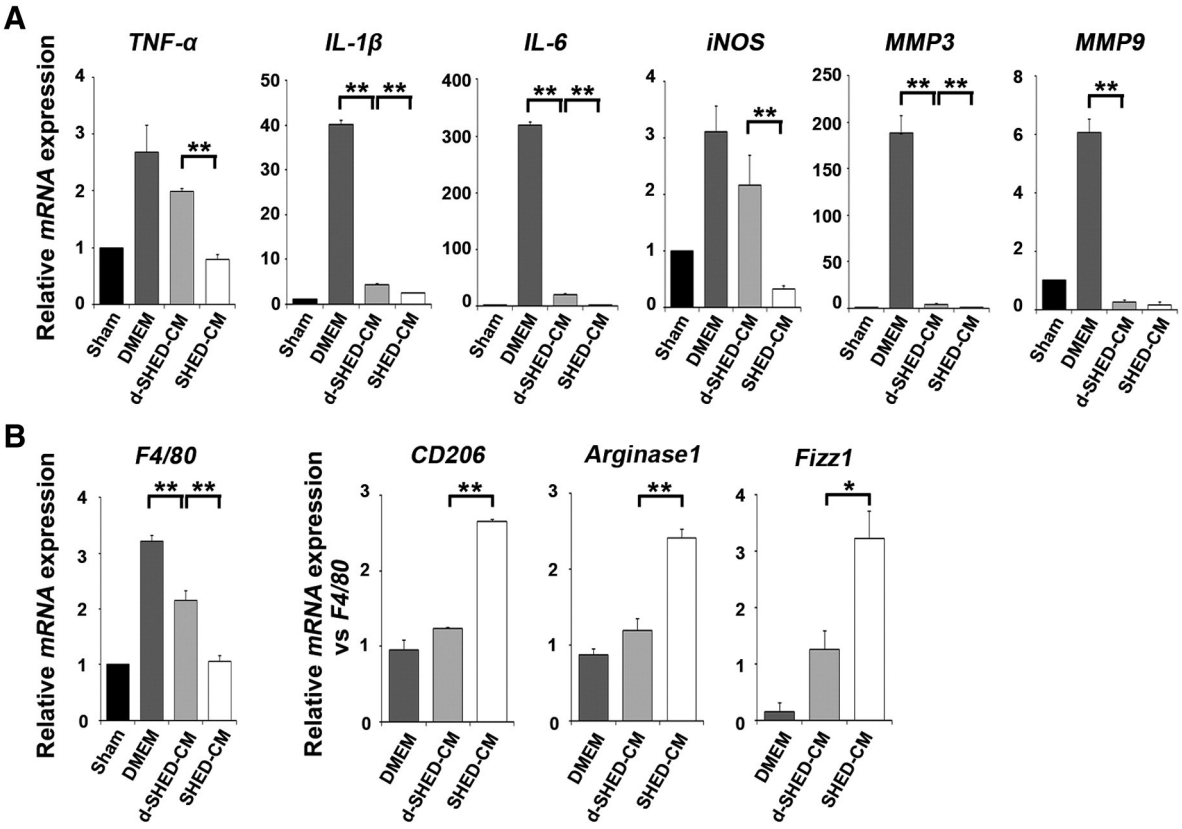

Fig. 6. d-SHED-CM fails to induce anti-inflammatory M2 circumstances in CAIA Gene expressions in the paws of DMEM-, d-SHED-CM-, and SHED-CM-treated mice on day 7 ($n = 5$ per group). Data represent the mean ± SEM; $^{*}p < 0.05$, $^{**}p < 0.01$. (A) Pro-inflammatory cytokine (*TNF-α*, *IL-1β*, *IL-6*), *iNOS*, and *MMP* gene expressions. Gene expressions were normalized to that of the sham group. (B) *F4/80*, a pan macrophage marker and M2-related marker (*CD206*, *Arginase1*, and *Fizz1*) gene expressions. *F4/80* expression was normalized to that of the sham group, and M2-related marker expressions were normalized to the *F4/80* expression in each sample.

these findings support the notion that therapies promoting M1 to M2 macrophage polarization may provide therapeutic benefits in treating various intractable diseases.

The blockade of osteoclastogenesis is another promising therapeutic strategy for treating RA [6,39]. Our data suggest that SHED-CM inhibited osteoclast differentiation through at least two mechanisms. SHED-CM inhibited the abnormally high articular RANKL expression, which mediates the osteoclastogenesis and bone destruction in CAIA. Several inflammatory cytokines abundant in the synovial fluid and synovium of RA patients can induce RANKL expression on SFs (synovial fibroblasts) resulting in increased RANKL signaling [40,41]. Our data revealed that SHED-CM suppressed the expression of genes that are upregulated in activated SFs, including *RANKL*, *MMP3*, and *MMP9*, indicating that SHED-CM may indirectly suppress osteoclast differentiation by inhibiting SF activation. Notably, the down-regulation of RANKL is unique to SHED-CM, but not BMSC-CM. We speculate that SHED-CM-induced synovial M2 macrophages exert a peculiar activity that abolishes RANKL on SFs. The detail mechanisms of the regulation of the RANKL expression by SHED-CM must be clarified in future study.

SHED-CM may also inhibit osteoclastogenesis directly, through the activity of OPG. A previous study suggested that BMSCs inhibit osteoclast differentiation through OPG production [29]. Here we showed that

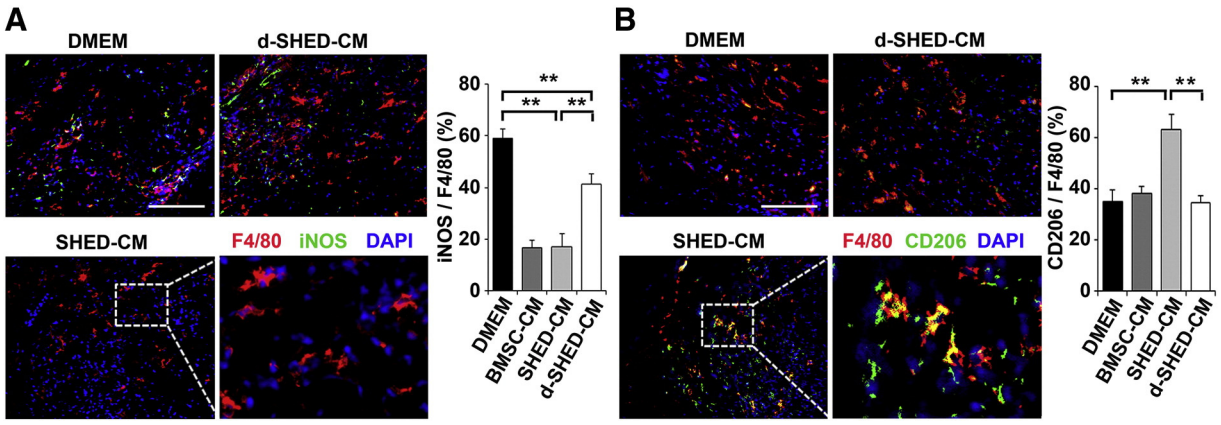

Fig. 7. SHED-CM reduces M1 but increases M2 macrophages in the joint synovium. (A, B) Representative immunohistological images and quantification of the joint synovial macrophages on day 7 ($n = 5$ per group). (A) $iNOS^{+}F4/80^{+}$ M1 macrophages and (B) $CD206^{+}F4/80^{+}$ M2 macrophages of DMEM, d-SHED-CM, SHED-CM. Boxed areas highlight macrophages of the SHED-CM group. Data represent the mean ± SEM; $^{**}p < 0.01$. Bar = 100 μm.

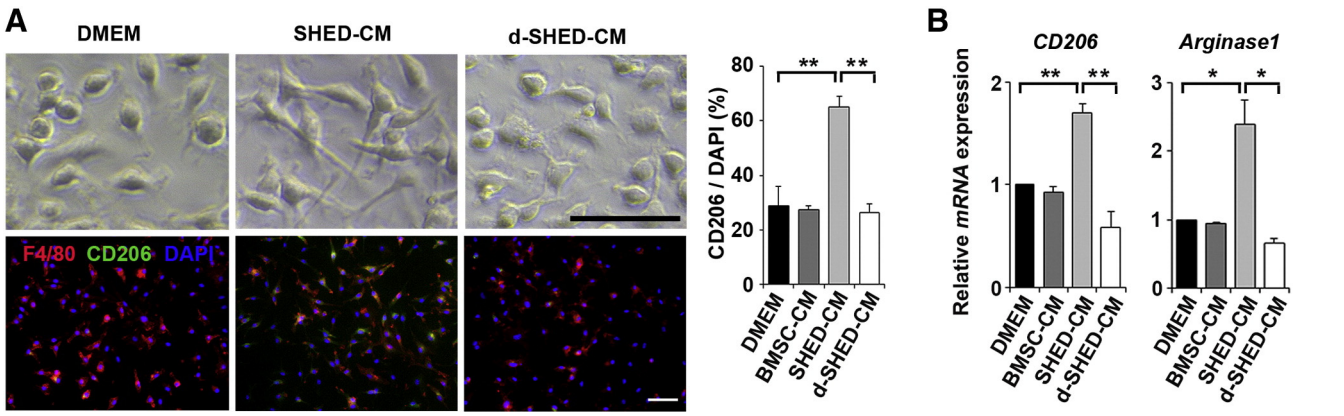

Fig. 8. SHED-CM induces M2 macrophages *in vitro*. *In vitro* M2 induction assay with BMCs. (A) Representative images of BMCs treated with DMEM, SHED-CM, or d-SHED-CM. Top; optical microscopic images, bottom; immunostaining images with F4/80, CD206, DAPI. right; quantification of $CD206^{+}DAPI^{+}$ macrophages ($n = 5$ per group). Data represent the mean ± SEM; $^{**}p < 0.01$. Bar = 50 μm. (B) Expressions of M2 macrophage-related genes, *CD206* and *Arginase1*, of BMCs ($n = 5$ per group). Results were relative to DMEM treatment. Data represent the mean ± SEM; $^{*}p < 0.05$, $^{**}p < 0.01$.

SHED-CM inhibited *in vitro* osteoclastogenesis more potently than BMSC-CM did, and found that OPG was present in SHED-CM at 2.8 times the level in BMSC-CM (Fig. 3). Thus, OPG may play a role in the SHED-CM-mediated suppression of osteoclastogenesis. Taken together, our data suggest that SHED-CM inhibits osteoclast differentiation and subsequent bone destruction through direct and indirect mechanisms.

In conclusion, here we showed that SHED-CM contained multiple therapeutic factors with the potential for treating CAIA. Importantly, we did not observe any adverse effects during the experimental treatment period. Our findings suggest that SHED-CM inhibited inflammation, induced M2-type conditions, and suppressed osteoclastogenesis and bone destruction in CAIA. Thus, SHED-CM may provide a novel anti-inflammatory and reparative therapy for patients with RA.

Funding

This work was supported by Grants-in-Aid for Scientific Research on Priority Areas from the Ministry of Education, Culture, Sports, Science, and Technology of Japan (22390372).

Conflicts of interests

None.

Acknowledgments

We are grateful to Y. Kobayashi (Matsumoto Dental University) for critical reading of the manuscript. We also thank the Division of Experimental Animals and Medical Research Engineering, Nagoya University Graduate School of Medicine, for housing the animals and for microscope maintenance.

References

[1] G. Firestein, Evolving concepts of rheumatoid arthritis, Nature 423 (2003) 356–361.
[2] D.L. Scott, F. Wolfe, T.W. Huizinga, Rheumatoid arthritis, Lancet 376 (2010) 1094–1108.
[3] A. Sica, A. Mantovani, Macrophage plasticity and polarization: in vivo veritas, J. Clin. Invest. 122 (2012) 787–795.
[4] S. Gordon, F.O. Martinez, Alternative activation of macrophages: mechanism and functions, Immunity 32 (2010) 593–604.
[5] P.J. Murray, J.E. Allen, S.K. Biswas, et al., Macrophage activation and polarization: nomenclature and experimental guidelines, Immunity 41 (2014) 14–20.
[6] H. Takayanagi, Osteoimmunology and the effects of the immune system on bone, Nat. Rev. Rheumatol. 5 (2009) 667–676.
[7] S.K. Brancato, J.E. Albina, Wound macrophages as key regulators of repair: origin, phenotype, and function, Am. J. Pathol. 178 (2011) 19–25.
[8] F. Djouad, C. Bouffi, S. Ghannam, D. Noel, C. Jorgensen, Mesenchymal stem cells: innovative therapeutic tools for rheumatic diseases, Nat. Rev. Rheumatol. 5 (2009) 392–399.
[9] A. Tyndall, Mesenchymal stem cell treatments in rheumatology: a glass half full? Nat. Rev. Rheumatol. 10 (2014) 117–124.
[10] A. Augello, R. Tasso, S. Negrini, R. Cancedda, G. Pennesi, Cell therapy using allogeneic bone marrow mesenchymal stem cells prevents tissue damage in collagen-induced arthritis, Arthritis Rheum. 56 (2007) 1175–1186.
[11] B. Zhou, J. Yuan, Y. Zhou, et al., Administering human adipose-derived mesenchymal stem cells to prevent and treat experimental arthritis, Clin. Immunol. 141 (2011) 328–337.
[12] Y. Liu, R. Mu, S. Wang, et al., Therapeutic potential of human umbilical cord mesenchymal stem cells in the treatment of rheumatoid arthritis, Arthritis Res. Ther. 12 (2010) R210.
[13] M. Chen, W. Su, X. Lin, et al., Adoptive transfer of human gingiva-derived mesenchymal stem cells ameliorates collagen-induced arthritis via suppression of Th1 and Th17 cells and enhancement of regulatory T cell differentiation, Arthritis Rheum. 65 (2013) 1181–1193.
[14] S. Gronthos, M. Mankani, J. Brahim, P.G. Robey, S. Shi, Postnatal human dental pulp stem cells (DPSCs) in vitro and in vivo, Proc. Natl. Acad. Sci. U. S. A. 97 (2000) 13625–13630.
[15] S. Gronthos, J. Brahim, W. Li, et al., Stem cell properties of human dental pulp stem cells, J. Dent. Res. 81 (2002) 531–535.
[16] M. Miura, S. Gronthos, M. Zhao, et al., SHED: stem cells from human exfoliated deciduous teeth, Proc. Natl. Acad. Sci. U. S. A. 100 (2003) 5807–5812.
[17] K. Sakai, A. Yamamoto, K. Matsubara, et al., Human dental pulp-derived stem cells promote locomotor recovery after complete transection of the rat spinal cord by multiple neuro-regenerative mechanisms, J. Clin. Invest. 122 (2012) 80–90.
[18] C. Gandia, A. Arminan, J.M. Garcia-Verdugo, et al., Human dental pulp stem cells improve left ventricular function, induce angiogenesis, and reduce infarct size in rats with acute myocardial infarction, Stem Cells 26 (2008) 638–645.
[19] T. Yamaza, A. Kentaro, C. Chen, et al., Immunomodulatory properties of stem cells from human exfoliated deciduous teeth, Stem Cell Res. Ther. 1 (2010) 5.
[20] T. Inoue, M. Sugiyama, H. Hattori, H. Wakita, T. Wakabayashi, M. Ueda, Stem cells from human exfoliated deciduous tooth-derived conditioned medium enhance recovery of focal cerebral ischemia in rats, Tissue Eng. Part A 19 (2013) 24–29.
[21] M. Yamagata, A. Yamamoto, E. Kako, et al., Human dental pulp-derived stem cells protect against hypoxic–ischemic brain injury in neonatal mice, Stroke 44 (2013) 551–554.
[22] F.M. de Almeida, S.A. Marques, S. Ramalho Bdos, et al., Human dental pulp cells: a new source of cell therapy in a mouse model of compressive spinal cord injury, J. Neurotrauma 28 (2011) 1939–1949.
[23] Z. Taghipour, K. Karbalaie, A. Kiani, et al., Transplantation of undifferentiated and induced human exfoliated deciduous teeth-derived stem cells promote functional recovery of rat spinal cord contusion injury model, Stem Cells Dev. 21 (2012) 1794–1802.
[24] A. Yamamoto, K. Sakai, K. Matsubara, F. Kano, M. Ueda, Multifaceted neuro-regenerative activities of human dental pulp stem cells for functional recovery after spinal cord injury, Neurosci. Res. 78 (2014) 16–20.
[25] K. Matsubara, Y. Matsushita, K. Sakai, et al., Secreted ectodomain of sialic acid-binding Ig-like lectin-9 and monocyte chemoattractant protein-1 promote recovery after rat spinal cord injury by altering macrophage polarity, J. Neurosci. 35 (2015) 2452–2464.
[26] A.R. Pettit, H. Ji, D. von Stechow, et al., TRANCE/RANKL knockout mice are protected from bone erosion in a serum transfer model of arthritis, Am. J. Pathol. 159 (2001) 1689–1699.
[27] T. Kawamoto, Use of a new adhesive film for the preparation of multi-purpose fresh-frozen sections from hard tissues, whole-animals, insects and plants, Arch. Histol. Cytol. 66 (2003) 123–143.
[28] S.L. Watson, H. Marcal, M. Sarris, N. Di Girolamo, M.T. Coroneo, D. Wakefield, The effect of mesenchymal stem cell conditioned media on corneal stromal fibroblast wound healing activities, Br. J. Ophthalmol. 94 (2010) 1067–1073.

[29] K. Oshita, K. Yamaoka, N. Udagawa, et al., Human mesenchymal stem cells inhibit osteoclastogenesis through osteoprotegerin production, Arthritis Rheum. 63 (2011) 1658–1667.
[30] F.Y. McWhorter, T. Wang, P. Nguyen, T. Chung, W.F. Liu, Modulation of macrophage phenotype by cell shape, Proc. Natl. Acad. Sci. U. S. A. 110 (2013) 17253–17258.
[31] K. Okunishi, M. Dohi, K. Fujio, et al., Hepatocyte growth factor significantly suppresses collagen-induced arthritis in mice, J. Immunol. 179 (2007) 5504–5513.
[32] S. Sarkar, X. Zhou, S. Justa, S. Bommireddy, Interleukin-22 reduces the severity of collagen-induced arthritis in association with increased levels of interleukin-10, Arthritis Rheum. 65 (2013) 960–971.
[33] L. Joosten, M. Helsen, F. van de Loo, W. van den Berg, Anticytokine treatment of established type II collagen-induced arthritis in DBA/1 mice: a comparative study using anti-TNFalpha, anti-IL-1alpha/beta and IL-1Ra, Arthritis Rheum. 58 (2008) 22.
[34] T. Takahashi, S. Katsuta, Y. Tamura, et al., Bone-targeting endogenous secretory receptor for advanced glycation end products rescues rheumatoid arthritis, Mol. Med. 19 (2013) 183–194.
[35] H. Lin, M.-D. Ah Kioon, C. Lalou, et al., Protective role of systemic furin in immune response-induced arthritis, Arthritis Rheum. 64 (2012) 2878–2886.
[36] K.M. Stuhlmeier, Aspects of the biology of hyaluronan, a largely neglected but extremely versatile molecule, Wien. Med. Wochenschr. 156 (2006) 563–568.
[37] I. Secundino, A. Lizcano, K.M. Roupe, et al., Host and pathogen hyaluronan signal through human siglec-9 to suppress neutrophil activation, J. Mol. Med. (Berl) (2015)http://dx.doi.org/10.1007/s00109-015-1341-8.
[38] H. Wakayama, N. Hashimoto, Y. Matsushita, et al., Factors secreted from dental pulp stem cells show multifaceted benefits for treating acute lung injury in mice, Cytotherapy 17 (2015) 1119–1129.
[39] Y. Choi, J.R. Arron, M.J. Townsend, Promising bone-related therapeutic targets for rheumatoid arthritis, Nat. Rev. Rheumatol. 5 (2009) 543–548.
[40] H. Takayanagi, H. Iizuka, T. Juji, et al., Involvement of receptor activator of nuclear factor kappaB ligand/osteoclast differentiation factor in osteoclastogenesis from synoviocytes in rheumatoid arthritis, Arthritis Rheum. 43 (2000) 259–269.
[41] E.M. Gravallese, C. Manning, A. Tsay, et al., Synovial tissue in rheumatoid arthritis is a source of osteoclast differentiation factor, Arthritis Rheum. 43 (2000) 250–258.